

Effects of Bears on Rockshelter Sediments at Tanay Sur-les-Creux, Southwestern Switzerland

Luc Braillard,¹ Michel Guélat,² and Philippe Rentzel²

¹*Institute of Geology and Palaeontology, Péroilles, University of Fribourg, 1700 Fribourg, Switzerland*

²*Institute of Prehistory, Geoarchaeology, University of Basel, Spalenring 145, 4055 Basel, Switzerland*

Sur-les-Creux rockshelter is located in the Prealps of southwestern Switzerland. The sequence of deposits in the rockshelter is 80 cm thick and consists of weathered gravels in a phosphate-rich matrix. A few Middle Palaeolithic artifacts and the bones of cave bear (*Ursus spelaeus*) were recorded in the fill. We present the results of sedimentological, geochemical, and micromorphological analyses of the rockshelter sediment. All analyses suggest an endokarstic origin of the sediments. The alteration cortices of the gravels imply *in situ* weathering over a long period. The phosphates are essentially biogenic and have an apatitelike nature. Phosphatization and intense mixing of the sediment are attributed to cave bear (digging of lairs, input of excrements, and carcasses). Only rare carnivore coprolites (lynx) were preserved in the cave deposits. © 2004 Wiley Periodicals, Inc.

INTRODUCTION

Excavations carried out since the 19th century in the caves of the Alpine region and the Jura mountains show that Pleistocene faunal remains are commonly embedded in phosphate-rich sediments. This was recognized early by researchers and discussed frequently in the context of site analyses (Kyrle, 1923; Abel and Kyrle, 1931; Koby, 1938; Schmid, 1958). The demand for fertilizers after World War I led to intensive mining of cave infillings and their Ca-phosphates in Austria. Examinations of the chemical composition of cave infillings were first carried out in the early 20th century in this context. There are also accounts of the extraction of cave fertilizers from the beginning of the 19th century in Germany (Bögli, 1980), Eastern Europe (Trimmel, 1968), and North America (Douglas, 1964).

The Drachenhöhle near Mixnitz in Styria (Austria) is one of the most well-known locations of phosphate mining for fertilizers. Besides 25,000 m³ of phosphatized sediments, the cave also yielded a rich cave bear (*Ursus spelaeus*) fauna (Abel and Kyrle, 1931). In his geochemical analyses, Schadler (1931) detected 8–15% P₂O₅ and made interesting observations on the origin of the Ca-phosphates. He concluded that the phosphates were more likely from bat guano than from carcasses or coprolites of cave bears. Shortly thereafter, Dubois and Stehlin (1933) published

the results of geochemical analyses of the sediment as part of palaeontological research on Middle Palaeolithic layers located in the cave of Cotencher (Switzerland). The two authors showed that the phosphate content in the sediments with cave bear remains could reach up to 12% P₂O₅ and was associated with reddish-brown phosphatic concretions. This was confirmed in further examinations (Schmid, 1958). Comparable evidence of corroded limestones encrusted with phosphates was detected by Lequatre (1966) in the Mousterian levels of the Grotte de Prélétang in the Vercors (France). This evidence, as well as the phosphates-rich deposits in the cave bear layers of the Wildkirchli, Appenzell (Switzerland), was seen to be the result of bear occupation (Schmid, 1961).

More recent archaeological excavations at Western European sites have demonstrated multiple origins and diagenesis of cave phosphates. Various pseudomorphic and neo-formed phosphates were detected in the deposits of the Caune de l'Arago in Tautavel (France). Their mineralogical or structural characteristics, however, did not allow conclusions to be drawn on the origin of these phosphates (Perrenoud, 1993). Van Vliet-Lanoë (1986), and Giresse and Van Vliet-Lanoë (1986) arrived at different conclusions from their micromorphological and geochemical analyses on the phosphate neo-formations within the Pleistocene fissure infilling at La Cotte St. Brelade (Channel Islands, England). With regard to the origin of the diagenetically formed phosphates, it was possible to prove that these stemmed from bone, bird guano, or organic phosphorus in ashes. Phosphatized yellow breccias are also known from the large cave infilling of Westbury-sub-Mendip, Southern England, where Macphail and Goldberg (1999) showed that a large part of the phosphates stem from weathered mammal bones and from bird guano. Finally, it could also be demonstrated that, for the Middle Palaeolithic horizons of Gorham's Cave and also partly for Vanguard Cave (Gibraltar), phosphate mineralizations hold an important position within the depositional processes (Macphail and Goldberg, 2000). In this case, the authors drew the conclusion that the origin of the phosphates can be traced back to guano of predatory birds and to the input of organic phosphorus. Detailed analyses on the genesis of phosphates in the Middle Pleistocene cave infillings of Pontnewydd Cave (Wales) were published by Jenkins (1994). He was able to prove a vertical translocation of Ca-Fe-phosphates from weathered layers containing fossils.

The examples listed above show that cave phosphates have generated intensive research for a long time, with emphasis on their origin, history of formation, and diagenetic transformations. These aspects of phosphates are considered in our study of the Sur-les-Creux rockshelter. The results of micromorphological, geochemical, and mineralogical analyses shed light on the origin and post-depositional modification of sediments at Sur-les-Creux, and are important to understanding site-formation processes in this and similar rockshelters.

GEOGRAPHICAL AND GEOLOGICAL CONTEXT

Sur-les-Creux rockshelter is located in the calcareous Prealps, SW Switzerland, 1.5 km northwest of the Tanay Lake, at an elevation of 1860 m (Figure 1). It was

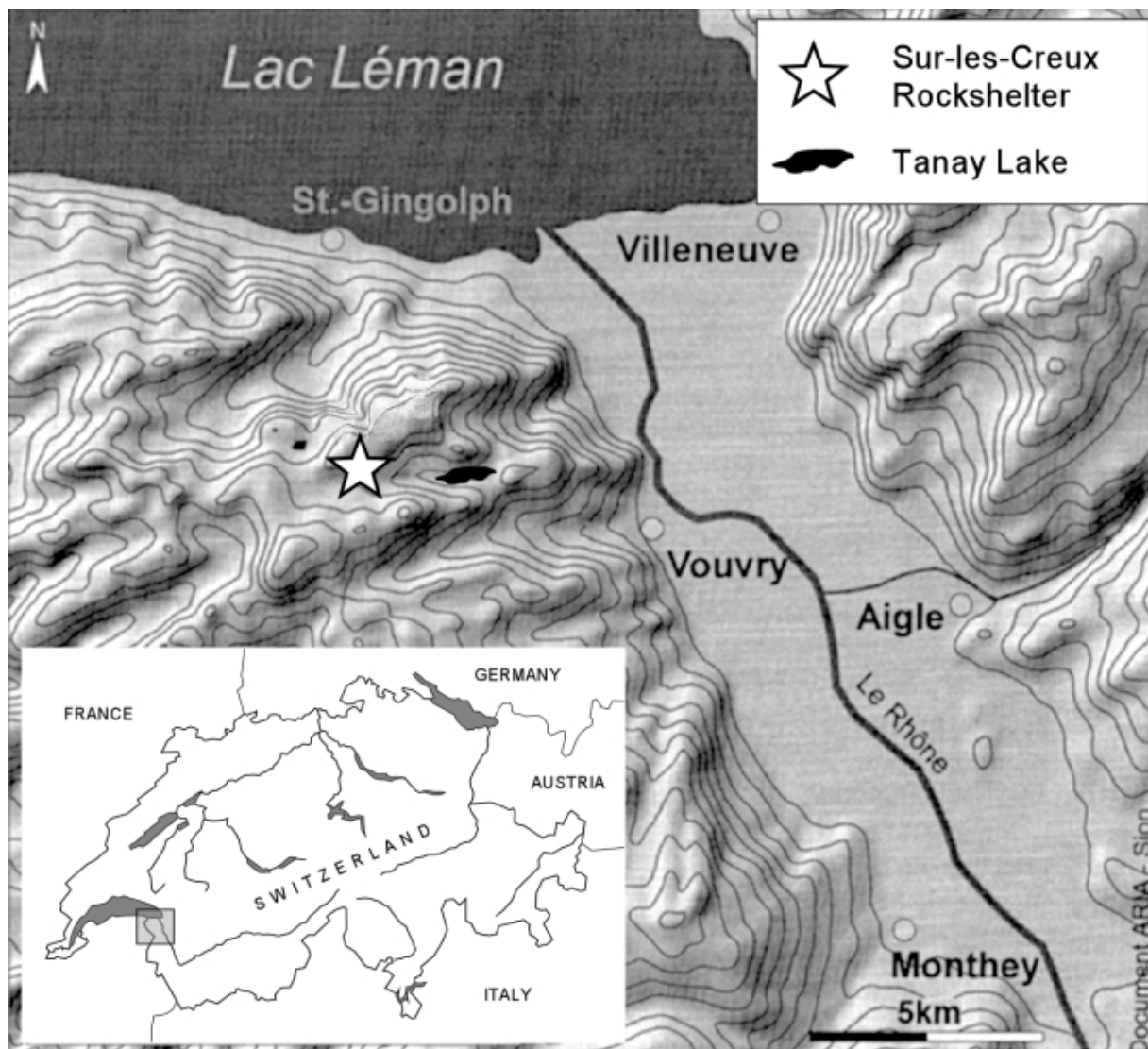


Figure 1. Topographic map showing the location of Sur-les-Creux rockshelter. The inset map shows the location of the study area in southwestern Switzerland.

eroded out of massive Malm limestones forming the northern side of an east-west trending hanging valley, perpendicular to the large Rhone Valley (Figure 2). The rockshelter opens towards the south. The amount of annual precipitation is high, between 2000 and 2400 mm, with snow cover from December to April.

There are several geological formations present in the vicinity of the site (Badoux et al., 1960). Lias outcrops occur 200 m northwest of the rockshelter and consist of siliceous limestones with chert nodules at the base and crinoidal limestones at the top. The Upper Jurassic massive limestones (Malm) form the framework of the whole range. They also form the cliff overhanging the site, which is probably the result of an east–west-oriented tectonic fault network covering the area. The limestones are deeply karstified, as shown by the numerous caves and galleries present in the vicinity. The walls of the rockshelter (Figure 3) display microfacies varying between oobiomicroite and oosparite, without micas or quartz. Tertiary argillaceous



Figure 2. General view of Sur-les-Creux rockshelter (see arrows).

limestones (*couches rouges*) cover a small syncline situated 150 m north of the site. During the last glaciation, the maximum elevation of the Rhône glacier was 1600 m (Badoux et al., 1960), or 250 m below the rockshelter, but a small local glacier flowing eastward was probably present in the Tanay valley. Indeed, local moraines cover the bottom of the valley, while talus cones accumulate at the base of the Malm cliffs.



Figure 3. Detailed view of Sur-les-Creux rockshelter. The height of the cliff is 6 m.

STRATIGRAPHY

The filling of the rockshelter, which varies in thickness from 60 to 80 cm, is composed of four main layers (Figures 4 and 5). Archaeological investigations revealed 12 artifacts (lithic and organic), as well as teeth and bones, mainly from cave bears, but also from ibex, chamois, reindeer, and lynx. The bones are present throughout the whole profile but in larger quantities in layer 3, where the artifacts were found (Praz et al., 2000).

Layer 1 is subdivided into two parts. The top (15 cm) is a rendzina composed of humic, granular, dark brown silts (~50%). They contain fine gravels and rare angular, slightly corroded limestones cryoclasts (~50%). The matrix is only slightly reactive to HCl. Roots are frequent throughout this horizon. The base (10 cm) is composed of pebbles and rare subrounded calcareous gravels (~60%) in a brown to light gray matrix (~40%) that is slightly less humic than the top horizon. No real stratification was observed, but oblate elements are horizontally arranged. The matrix is slightly reactive to HCl. The gravels are more corroded than those in the top, especially their upper sides, implying *in situ* alteration.

Layer 2 (15 cm) is composed of gravels (average diameter: 4–5 cm) and rare rounded pebbles in a light brown to yellow silty clay matrix (~40%) that reacts strongly to HCl. Preferred orientation of gravels and good sorting of the elements indicate an alluvial endokarstic deposit.

Layer 3 (15–45 cm) includes rounded and corroded gravels and fine gravels with a particularly pronounced alteration of the upper sides. The sorting of the elements (average diameter: 3–4 cm) is quite good, but no stratification is present. The gravels (~35%) are matrix-supported in a compact light brown to yellow silty clay (~65%) that reacts strongly to HCl.

Layer 4 (1–5 cm) is composed of yellow-orange, very compact and very clayey silts (~90%). It contains rare, slightly corroded gravels and fine gravels (~10%). This layer fills the irregularities of the limestone substratum. It is a mixed sediment made of decarbonated clays and allochthonous karstic inputs that reacts strongly to HCl.

The four horizons have distinct to diffuse boundaries (except for the abrupt contact between layers 3 and 4), are generally horizontal, and dip slightly to the south. Layer 3 becomes significantly thicker from south to north. In the northern part of the shelter (meters 0 and –1, Figure 4), two new layers appear, also dipping to the south. They are sandier and seem contemporary to layer 2. Calcareous concretions occur towards the northern side-wall. This part of the profile remains humid. These observations suggest sediment input from an old karstic channel, currently sealed by the deposits. It is also possible that the rockshelter is a partly preserved chamber of an underground, east–west oriented gallery. This chamber may have been exposed with the erosion of the cliff.

METHODS

Four bulk samples were air-dried and prepared for conventional grain-size analyses of the sand and gravel fractions using sieves (Rivière, 1977; Hadjouis, 1987).

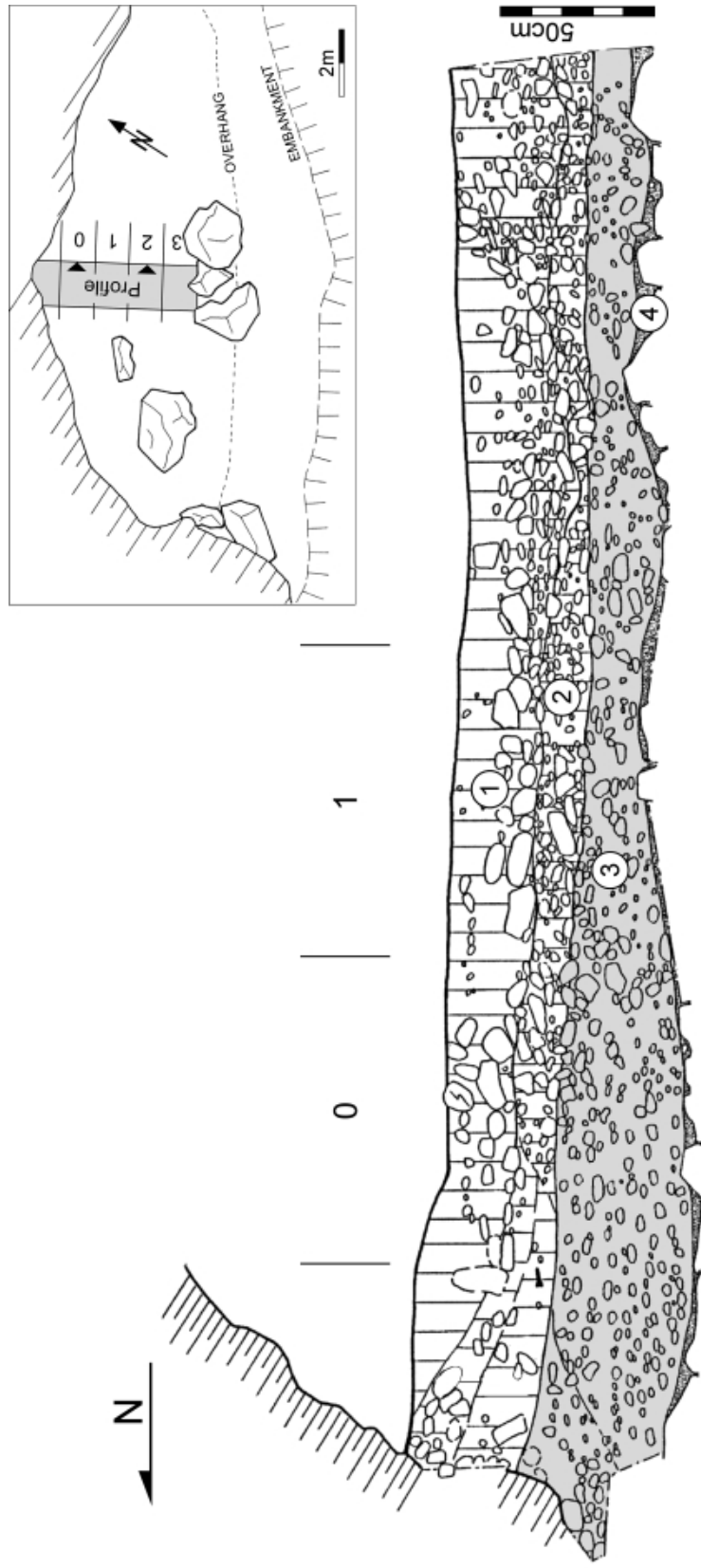


Figure 4. Stratigraphic section of the deposits in Sur-les-Creux rockshelter. Layer 3, in gray, contains many cave bear bones as well as Middle Palaeolithic artifacts. Phosphatization of the sediment and corrosion of limestone clasts is very intense in layers 3 and 4. The shape of the gravels is generally rounded. Numbers refer to layers as well as samples position.

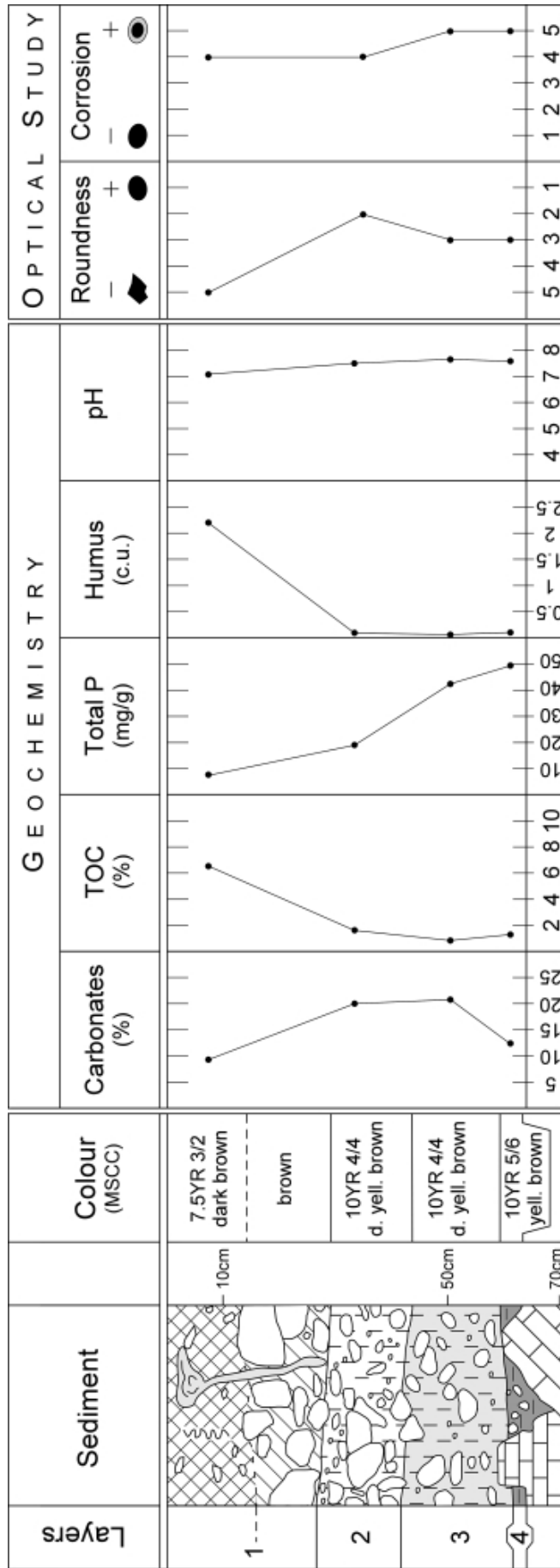


Figure 5. Stratigraphy and geochemistry of the deposits in Sur-les-Creux rockshelter. The results of optical analysis of the limestone clasts are shown on the right side of the diagram (for roundness and corrosion classes, see Figure 6 and Table I).

The silt and clay fractions were measured with a Laser system (Malvern, MS20). For each sample, the fraction smaller than 1 cm was examined with a binocular microscope to qualitatively and quantitatively estimate the different constituents. Corrosion (Table I) and shape (Figure 6) of the limestone clasts were also noted. Three routine measurements of the <0.5 mm sediment fraction were taken at the Geoarchaeological Laboratory of the University of Basle (Brochier and Joos, 1982). Total carbonate content was determined by production of carbonic gas after reaction with HCl (i.e., Müller's calcimeter). Humus content was determined by colorimetric method using sodium fluoride as a reagent, and pH was measured with a pH meter in a KCl solution. Phosphorus sequential extractions and analyses were conducted at the Geological Institute of the University of Neuchâtel, Switzerland, according to Ruttenberg (1992), Anderson and Delaney (2000), and Tamburini (2002). This method, originally used for marine deposits, is based on a selective dissolution of phosphates. It permits the identification of Fe-bound phosphates (by extraction in a sodium citrate, sodium bicarbonate, and sodium dithionite solution), biogenic phosphates of Ca F-apatite type (first sodium acetate, then magnesium chloride solution), detrital fraction (hydrochloric acid), and organic phosphates (hydrochloric acid, after combustion of the organic matter at 550°C). Total organic content (TOC), measured with a Rock-Eval 6 using the pyrolyse method (Espitalié et al., 1986; Lafargue et al., 1996), and X-ray diffraction (XRD) analyses, using a SCINTAG XRD 2000 diffractometer, were also conducted at the Geological Institute of the University of Neuchâtel. Bulk sediment compositions were determined by XRD based on methods described by Kübler (1983, 1987) and Adatte et al. (1996).

For the micromorphological study, a 31-cm-high monolith was encased in plaster-of-Paris during field work, then air-dried, impregnated with an acetone-diluted epoxy resin, and cut with a diamond saw. A series of six covered thin sections (4.5 cm × 4.5 cm) was prepared by Th. Beckmann, Braunschweig, Germany. Slides were examined optically on a Leitz DM-RXP microscope (using magnification of up to 630×) in plane-polarized light (PPL), crossed-polarized light (XPL), oblique-incident light (OIL), and using UV-fluorescence (UVL). Thin sections were described according to Bullock et al. (1985) and Courty et al. (1989).

It is important to note that only one column, in the center of the rockshelter, was sampled and examined. Lateral sampling control, which might have provided additional information, was, however, not implemented because of the small di-

Table I. Corrosion classes of limestone clasts.

Corrosion Class	Description
1 No corrosion	Sharp edges, fresh sides
2 Abraded clasts	Blunt edges, slightly abraded sides
3 Slightly corroded clasts	Very blunt edges, strongly abraded sides
4 Corroded clasts	Weak superficial decarbonatation, slightly porous sides, chalky feel
5 Strongly corroded clasts	Strong decarbonatation, porous and friable sides, chalky feel

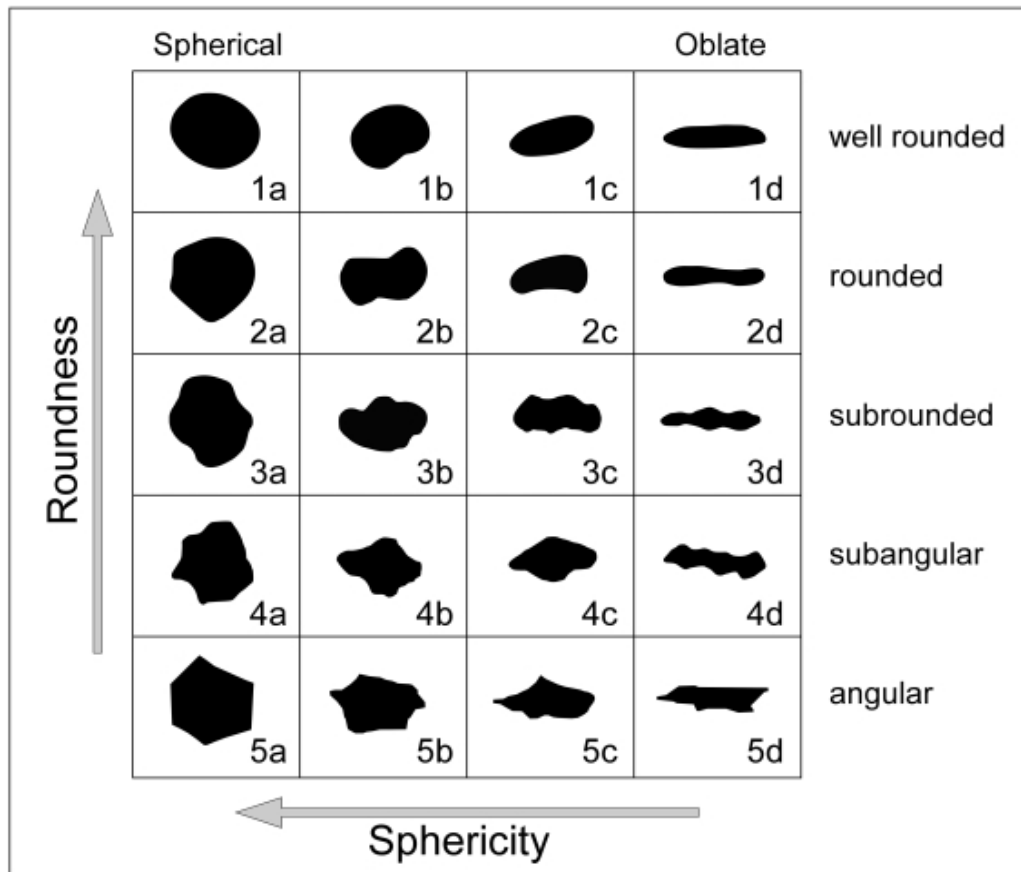


Figure 6. Definition of roundness (1–5) and sphericity (a–d) classes (modified from Bullock et al., 1985).

mensions of the rockshelter as well as the simple geometry and lateral homogeneity of the layers.

RESULTS

Granulometry

The cumulative curves (Figure 7) show that the sand fraction is very low in layers 1–3 but reaches 18% in layer 4. According to the binocular study and micromorphology, however, these sands are not single mineral grains but aggregates made of silt-sized particles (see below). If mechanical disaggregation of these aggregates had been performed before the grain-size analysis, layer 4 would appear better sorted in the silt fraction. The granulometric parameters of this basal bed should, therefore, not include the sand fraction, as shown in Table II (layer 4, silt + clay). The cumulative curves of layers 1 to 3 clearly point to a dominant gravel fraction. The intermediate appearance of layer 3 suggests the formation processes were between those operating in layer 1 (input of cryoclasts essentially) and those of layer 2 (input from the karst network).

Granulometric parameters such as sorting index (S_o) and skewness (S_k) clearly

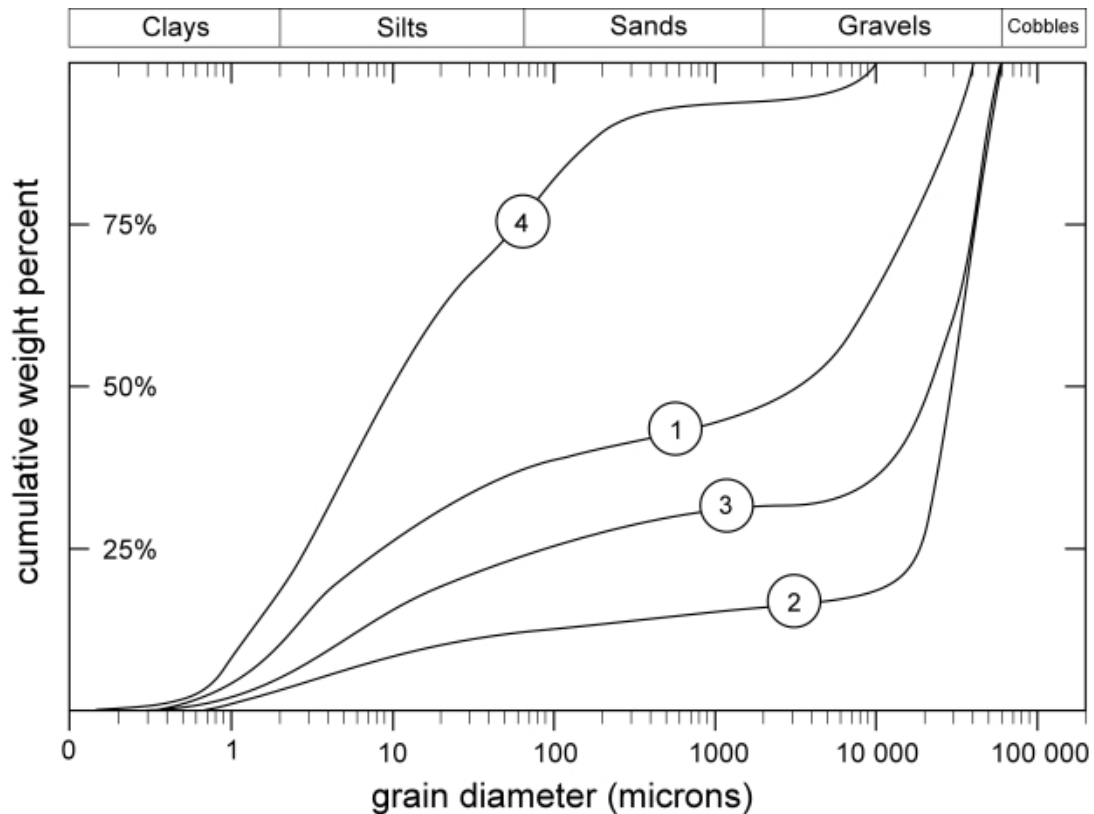


Figure 7. Graph showing grain-size distributions (cumulative curves) for samples from Sur-les-Creux rockshelter. The numbers refer to layers 1–4.

separate layers 1 and 3 from layers 2 and 4. Layers 2 and 4 (silts + clays) are characterized by a good sorting index and a very low skewness, which implies a selective transport agent, most likely a runoff process within an old karst network. According to Hjulström (1935), the speed of the current can be estimated to be about 1 m/s for the gravels of layer 2 and only 0.05 m/s for the fine fraction of layer 4.

Although the fine fraction of all layers contains quartz and micas, the median size ($<10 \mu\text{m}$) is too small to conclude that loess was deposited inside the rockshelter. A primary loess origin is possible, but a secondary sorting by endokarstic runoff must be invoked.

Table II. Grain-size parameters.

Layers	Q_1 (μm)	Q_3 (μm)	Md (μm)	So ^a	Sk ^a
1	20	14,000	3000	26.5	0.03
2	19,000	41,000	30,000	1.5	0.9
3	90	40,000	22,000	21.1	0.01
4	3	63	10	4.6	1.9
4 (silt + clay)	2	14	5.8	2.6	0.8

^a So: $(Q_3/Q_1)^{1/2}$; Sk: $Q_3 \times Q_1/Md^2$.

Optical Study of Hand Specimens

Composition of the Fill

Braillard (2000) conducted a detailed qualitative and quantitative study of sediments from the Sur-les-Creux rockshelter. The coarse fraction (>2 cm) is exclusively composed of Malm limestone clasts. Below this size, as seen under the binocular microscope, some allochthonous elements occur, mainly dark siliceous limestone and fine siliceous sandstone belonging to the Lias. These fragments, commonly angular, appear to be knapping waste. The less frequent subangular to rounded elements were transported by the karst network. Some small tertiary *couches rouges* fragments are also present and can also be attributed to a natural origin, since their suitability for artifact manufacturing is very low.

The largest part of the allochthonous material is brownish yellow, indurated silt aggregates. They represent as much as 90% of the fine fraction (<0.5 mm) and can reach 5 mm in diameter. These aggregates are made of silt-sized particles, mainly quartz and white mica, which are absent in the bedrock. The granulometric features of these silts indicate that they underwent post-depositional sorting. Although it is likely that these sediments were originally deposited above the shelter, they have three possible origins: loess, moraine deposits, or insoluble residue from the *couches rouges*.

The sand fraction of all samples contains bones and teeth fragments (1–4% in layers 1–3, and up to 20% in layer 4). The proportion of microcharcoal does not exceed 1%, except in layer 1 where it reaches 10%.

Shape and Corrosion of the Calcareous Clasts

The calcareous elements derived from the Malm limestones are angular and oblate (class 5c, see Figure 6) in the top of layer 1 (cryoclastic debris), and rounded to subrounded (classes 2b, 2c, 3b, 3c) in the rest of the profile (karstic input). All clasts of the profile are corroded. However, a stronger corrosion (class 5; see Table I) is observed within layer 3 when compared to layers 1 and 2 (class 4).

It is important to note that the roundness is more evident in layer 2 than in layer 3, even though the corrosion is more pronounced in the latter (Figure 5). Thus, the roundness of the clasts cannot be explained by alteration only. Consequently, the hypothesis that the clasts are rounded due to transport processes in karstic channels, already supported by petrographic and granulometric arguments, is supported by the lack of correlation between roundness and corrosion. The distance necessary to make calcareous gravels round is very low (Bögli, 1980), and they can lose up to half of their mass by abrasion over a distance of less than a 100 m in a karst network.

Two pebbles from the base of layer 1 were sectioned and examined. Both pebbles exhibited stronger corrosion on their upper sides. The whitish alteration cortex is 2 mm thick at the top, but measures only 0.5 mm at the base of the clasts. This is interpreted as a consequence of slightly acid fluids coming from the present-day humic horizon.

Geochemical Context

Layer 1 is different compared to the other layers in the rockshelter (Table II and Figure 5). It has abundant organic matter (TOC up to 6.5%) and characteristics that imply a plant or animal origin but not one from charcoal (hydrogen index: 199, oxygen index: 374). The humus level also is high in layer 1 (2.2 colorimetric units [c.u.]), whereas the carbonates are low (9%) compared to the other layers. Furthermore, pH approaches neutrality in layer 1. These results are typical of a leached soil, a rendzina, under the influence of the rhizosphere. The carbonate content is much higher in layers 2 and 3 (about 20%). In addition to the effects of dissolution at the surface, this increase is due to allochthonous inputs of calcite, as implied by the micromorphological analysis (described later). Layers 2 and 3 are also much lower in total organic matter (1.7% and 0.1%, respectively) and humus contents (0.1 c.u. and 0.05 c.u., respectively) than layer 1, while their pH levels are slightly higher. Also, layer 4 has a lower carbonate content (12%) than the layers 2 and 3.

The relatively high phosphorus values indicate the presence of phosphate in all layers. Phosphorous increases towards the bottom of the stratigraphic sequence (Table III); the phosphorus content in layer 4 (49.2 mg/g) is six times higher than in layer 1 (7.7 mg/g). It is important to note that an enrichment in bone fragments was observed by the binocular analysis of the sand fraction at the base of the profile. Nevertheless, the high concentrations of phosphorus cannot be solely explained by the presence of bone, particularly at the top of the profile (see below).

Phosphate Characterization

Speciation

The speciation analysis involved measurement of four phosphate fractions: the Fe-bound, biogenic, detrital, and organic phosphates. The results obtained for the four samples, which were also used for the geochemical analysis, are presented in Table IV. They support the conclusion that the increase in total phosphorus towards bottom of the stratigraphic sequence originates from the biogenic fraction. By considering each fraction relative to the total phosphate content of the sample, the proportion and origin of different phosphates types in the profile can be evaluated (Figure 8). Once again, the biogenic fraction represents the main fraction of the phosphates (from 70% in layer 1 to 80% in layer 4), and its variation is related to the other types. Phosphorus linked to organic matter is highest in layer 1 (9%) and

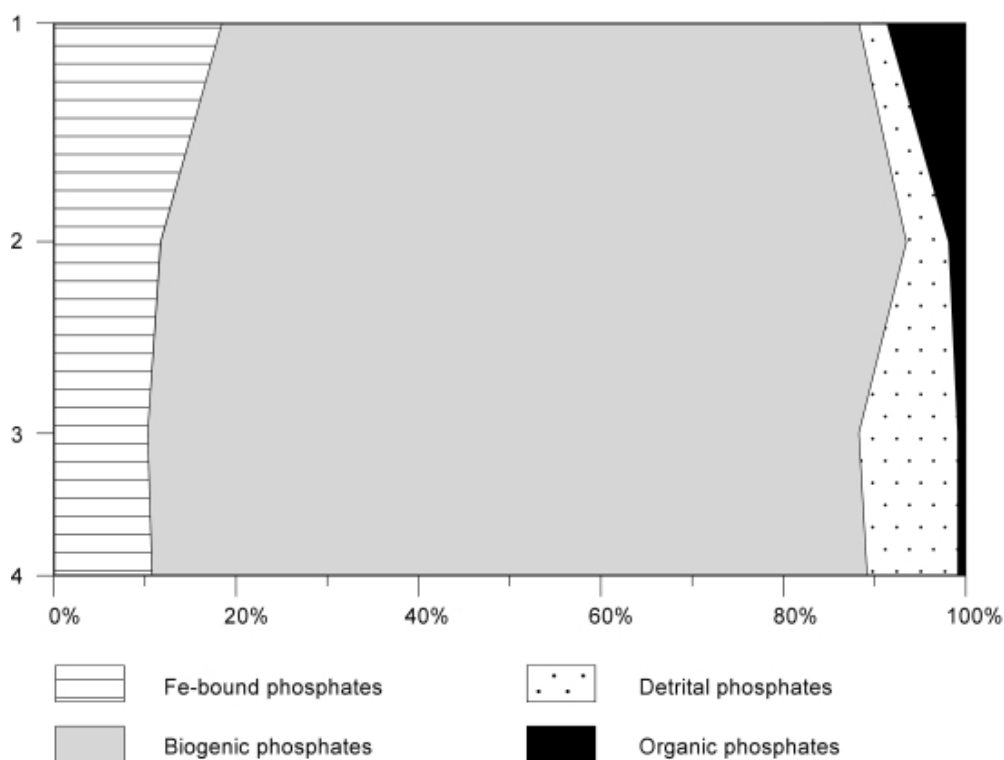
Table III. Results of geochemical analyses.

Layers	Carbonates (%)	TOC (%)	P Total (mg/g)	Humus (c.u.)	pH _{KCl}
1	9	6.5	7.7	2.2	7.1
2	20	1.7	18.8	0.1	7.5
3	21	0.9	42.5	0.05	7.7
4	12	1.4	49.2	0.1	7.6

Table IV. Results of phosphate speciation.

Layers	Fe-Bound		Biogenic		Detrital		Organic		Total	
	mg/g	%	mg/g	%	mg/g	%	mg/g	%	mg/g	%
1	1.4	18.5	5.4	69.8	0.2	3.1	0.7	8.6	7.7	100
2	2.2	11.7	15.4	81.8	0.9	4.6	0.4	1.9	18.8	100
3	4.4	10.3	33.2	78	4.6	10.8	0.4	0.9	42.5	100
4	5.3	10.8	38.6	78.4	4.9	9.9	0.5	0.9	49.2	100

decreases very rapidly towards the base of the profile (2% in layer 2 and 1% in layer 4). This confirms the results of the TOC analysis. The source of this organic fraction is the plant roots colonizing the upper part of the rockshelter fill, i.e., layer 1. The detrital fraction shows an inverse relation; it increases from the top (3% in layer 1) to the bottom (10% in layer 4) of the stratigraphic sequence. This result and the mineralogical data (discussed later) indicate that the detrital fraction is probably not due to allochthonous inputs. This kind of phosphate is related to the bone and teeth fragments contained in the sand fraction, particularly at the base of the stratigraphic sequence. The Fe-bound phosphates slightly decrease in the lower part of the profile (from 18.5% in layer 1 to 11% in layer 4). This type of phosphates should be diagenetic and may be attributed to the presence of hydroxides or clays within the sediment.

**Figure 8.** Phosphate speciation in layers 1–4 (for total phosphorus content, see Table IV).

Mineralogy

The X-Ray diffraction analysis performed on the four samples shows several peaks at around 2.8 Å, with the intensity of the peaks increasing from layer 1 to layer 4. The most distinct peak, at 2.79 Å, suggests a relatively well-crystallized phosphate similar to Ca F-apatite. The phosphates related to carbonates probably correspond to the biogenic fraction. As discussed earlier, this type is dominant compared to the other types of phosphates. In the case of caves and shelters, such cryptocrystalline varieties of apatite have often been designated as “collophane” (Deer et al., 1992).

The semiquantitative sediment analysis provides interesting additional information (Table V, Figure 9). First, the well-crystallized phosphates increase from the top (3%) to the bottom (9%) of the profile. This confirms the results of the geochemical analyses. The proportions of plagioclase and calcite are highest in layer 2 (9% and 19% respectively). As demonstrated by the micromorphological analysis, this can be explained by the abundance of washed silts that are rich in allochthonous minerals. Quartz content steadily decreases towards the bottom of the profile. Poorly crystallized phyllic minerals are especially abundant in layer 4, which may be related to the presence of limpid argillans and iron-hydroxide impregnations detected by microscopy.

Micromorphology

Six thin sections from layers 2, 3, and 4 were examined (Figure 10). The main observations and interpretations drawn from the micromorphological analysis are summarized in Table VI.

Alteration Cortex of Coarse Elements

Autochthonous lithic elements (Malm limestones) are essentially oobiomicroites. They show a particular alteration cortex, prevalent throughout layer 3 (Figure 10). In layer 2, the alteration is similar but less penetrating. The desquamation (flaking due to chemical weathering) zone is poorly marked and generally lacks phosphates. A white peripheral zone, parallel to the surface of the calcareous clasts and 1–5 mm thick, can be observed with the naked eye. The transition to the core of the clasts is characterized by a brownish zone 0.1–2 mm thick.

Table V. Results of the XRDA semiquantitative dosage, bulk sediment percentage (unoriented powder).

Layers	Quartz	Plagioclase	Calcite	Ca-Apatite	Others ^a
1	26.3	3.1	9.2	2.6	59
2	24.6	9.2	19.3	3.2	43.7
3	21.4	3.5	15.2	7.9	52
4	17.1	1.1	5.3	8.6	67.9

^aThe “Others” are mainly well-crystallized phyllosilicates.

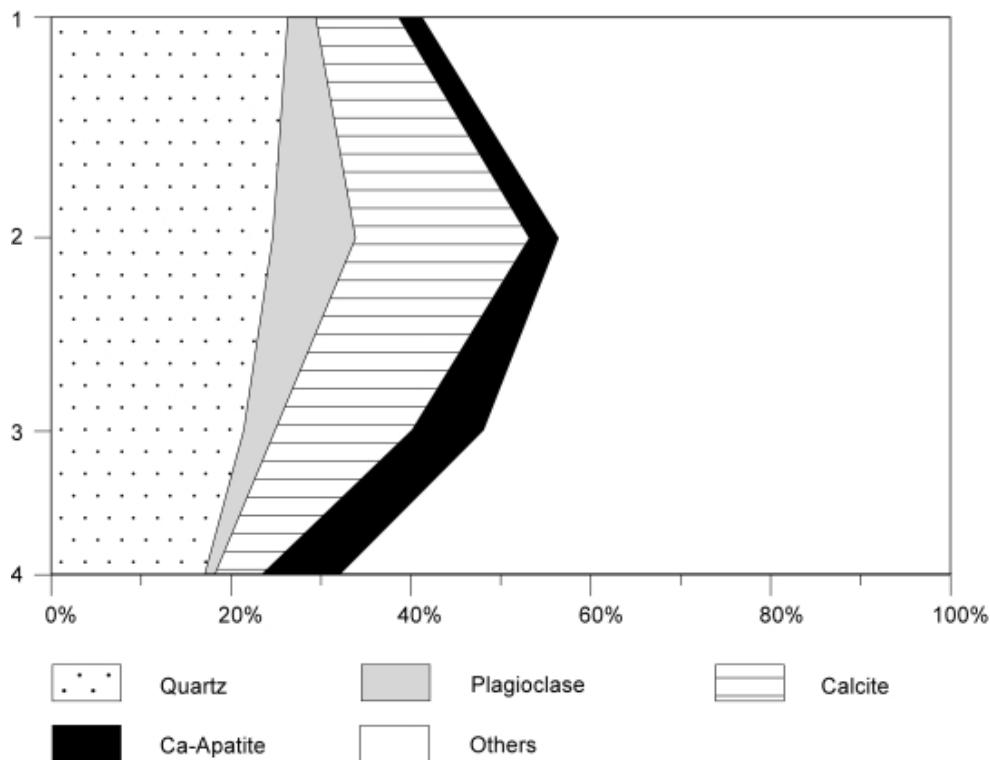


Figure 9. Results of XRD semiquantitative analysis of layers 1–4.

Under plane-polarized light, the whitish cortex appears darker than the core. This darker appearance results from impregnation by small, black particles (5–10 μm) that are most likely organic matter. The boundary to the desquamation zone is distinct, but the transition from the desquamation zone to the core is diffuse. This zone separating the cortex from the core is partially to totally dissolved (Figure 11), and yellow phosphate locally fills the voids. The bioclasts and calcite veins are not affected by dissolution. This cortex type is similar to the type 2 described in the sediments of the Gigny Cave (Campy, 1989), except that at Sur-les-Creux, the desquamation zone contains phosphates.

The alteration cortex of the lithic elements likely developed penecontemporaneously to the deposition of the rockshelter fill and suggests a history of relatively temperate humid phases (Campy, 1989). This argument corroborates the dating proposed by the artifacts and bones, i.e., a pre-Last Glacial Maximum (LGM) temperate interstade (Praz et al., 2000). Furthermore, layer 3 can be interpreted as the result of a period of slow, limited sedimentation, during which alteration cortices had enough time to develop. The variable degree of corrosion supports the interpretation that alteration occurred during deposition, not after burial, and could be the result of sediment mixing by bear making hibernation lairs. The formation of layer 2 was followed by a period of rapid sedimentation of karstic origin (layer 2).

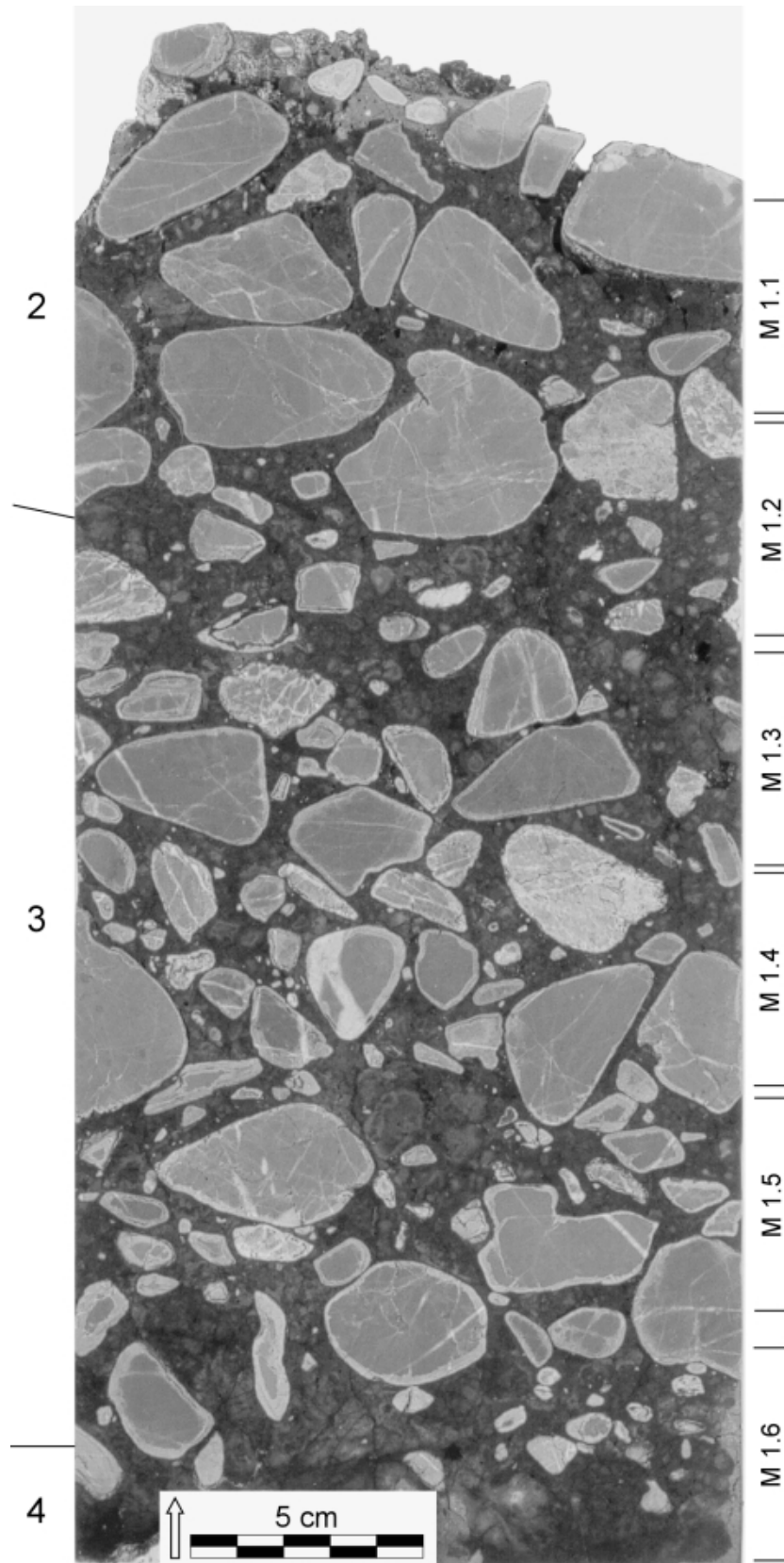


Figure 10. Vertical polished thin section through layers 2, 3, and 4 showing the deeply corroded clasts in layer 3. Thin section locations are indicated to the right.

Table VI. Summary of the micromorphological analysis of deposits in the Sur-les-Creux rockshelter.

Layer	Micromorphology	Interpretation
1	—	Humus bearing horizon with cryoclasts. Rendzina (Aca horizon)
2	Rounded and slightly corroded limestones. Matrix: yellow-brown clayey silt as in layer 3. Medium porosity (15–20%, cracks and channels), granular microstructure. Bone fragments commonly corroded. Crumbled coprolites. Silty to sandy illuviation (quartz, micas and calcite grains) as well as dusty intra-aggregate illuviations. Secondary carbonates. Roots. Diffuse lower boundary	Alluvial endokarstic deposit with a phosphatized matrix reworked from layer 3: — Freeze and thaw effect more pronounced than in layer 3 — Flushing — colonization by vegetation
3	Subrounded and deeply corroded limestones. Alteration cortex with phosphatized impregnations (internal quasi coating). Matrix: phosphatized yellow-brown clayey silt. Low porosity (10%, cracks and channels), blocky microstructure. Silty content much higher than in layer 4. Few siliceous clasts. Little corroded bone and teeth fragments. Dusty or limpid illuviations (several phases). Aggregates with concentric iron and manganese oxydes (internal quasi coating). Abrupt erosive lower boundary, some fragments being reworked from layer 4	Phosphatized condensed layer: — Erosion and endokarstic runoff deposits (gravels and fine fraction) — Enrichment in phosphates through animal excrements; percolations (temporary water table) homogenization by bears — Freeze and thaw (little pronounced) — Flushing
4	Yellow-brown to orange loamy silt with low porosity (5–10%, cracks and channels). Complex subangular blocky microstructure, partially reactivating a former platy structure. Some rounded cryoclasted aggregates. Few sand-size siliceous elements. Clayey isotropic groundmass impregnated with phosphates and covered with silty grains, mostly quartz and micas. Bone and teeth fragments, locally corroded. Coprolites of carnivores. Limpid argillan coatings overlayed by a washed and well sorted silty to sandy illuviation. Locally some iron oxide impregnation	Compound condensed layer: — Fine infilling of collapsed blocks — Enrichment in phosphates and bioturbation; percolations (suspended fine particules in a temporary water table) — Freeze and thaw — Flushing — Fissuration (blocky structure)

Components and Microstructure of the Matrix

Layer 4 consists of silt grains (~40%) in a brownish orange clay matrix (~60%). Angular and rounded quartz and white micas form most of the very well sorted silt fraction. In XPL, the matrix appears isotropic and phosphatized (Figure 12). Under PPL, there are localized red areas resulting from impregnation by iron oxides. Mi-

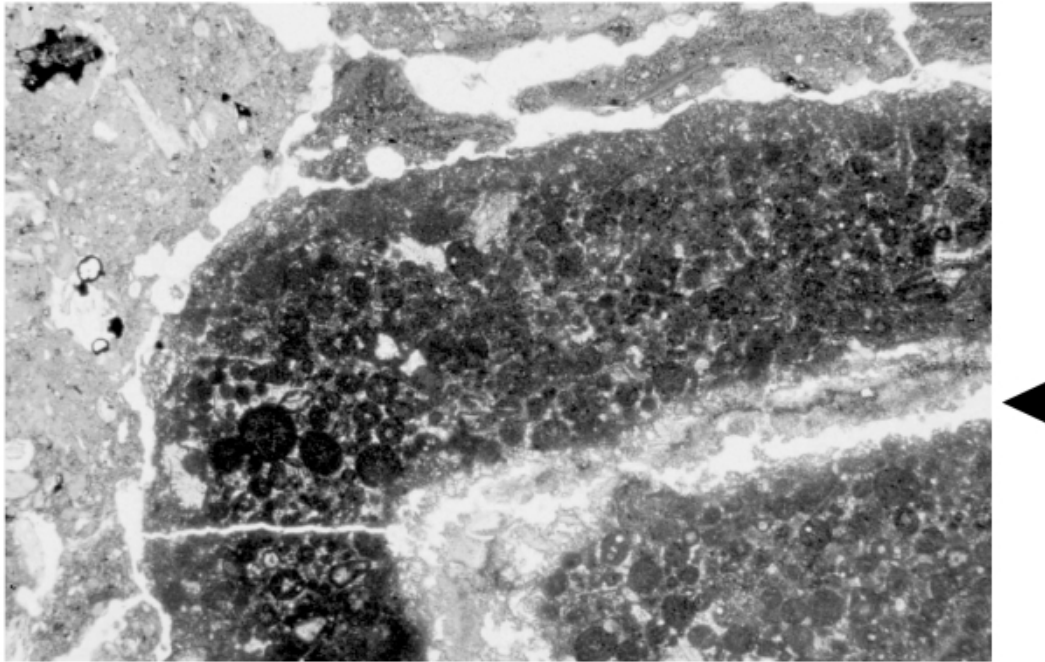


Figure 11. Photomicrograph showing the alteration cortex affecting the limestones of layer 3. The desquamation zone (flaking due to chemical weathering, see arrow) is parallel to the clast edge and partially filled with secondary phosphates. Thin section M1.5, PPL. Frame length is 4.4 mm.

nor components are bones and teeth fragments (<5%), as well as small particles that appear light brownish yellow in PPL and completely black in XPL (Figure 12). These particles are interpreted as fragments of carnivore coprolites composed of phosphatized gel and locally including small bone chips and mineral grains (P. Goldberg, personal communication, 2001). Osteological data suggest that the coprolites are from lynx.

In layer 4, millimeter-sized aggregates have polyhedral subangular microstructure and a porosity of 5–10%. Also, a former platy structure that may be attributed to freezing and thawing developed in this layer (Figure 13). This complex microfacies is difficult to interpret and seems to be the result of cryoclastic activity on the one hand, and of intense sediment mixing by bear activity on the other hand.

Layer 3 differs from layer 4 in color and texture. The brownish yellow clay matrix of layer 3 is less phosphatized and composes 30–40% of the deposits. However, the silt fraction (60–70%) in layer 3 is similar to the silt in layer 4. The boundary between layers 3 and 4, more clearly visible in XPL, is abrupt and appears to be an erosion surface (Figure 12). Reworked rounded aggregates from layer 4 are present at the bottom of layer 3. The minor components in layer 3 are similar to those in layer 4, but there are more coprolites and slightly corroded bones and teeth fragments in layer 3. The microstructure is polyhedral subangular, as in layer 4, but porosity is greater (10%) in layer 3. The inner microstructure of aggregates in layer 3 is complex and evolved before illuviation occurred (Figure 14).

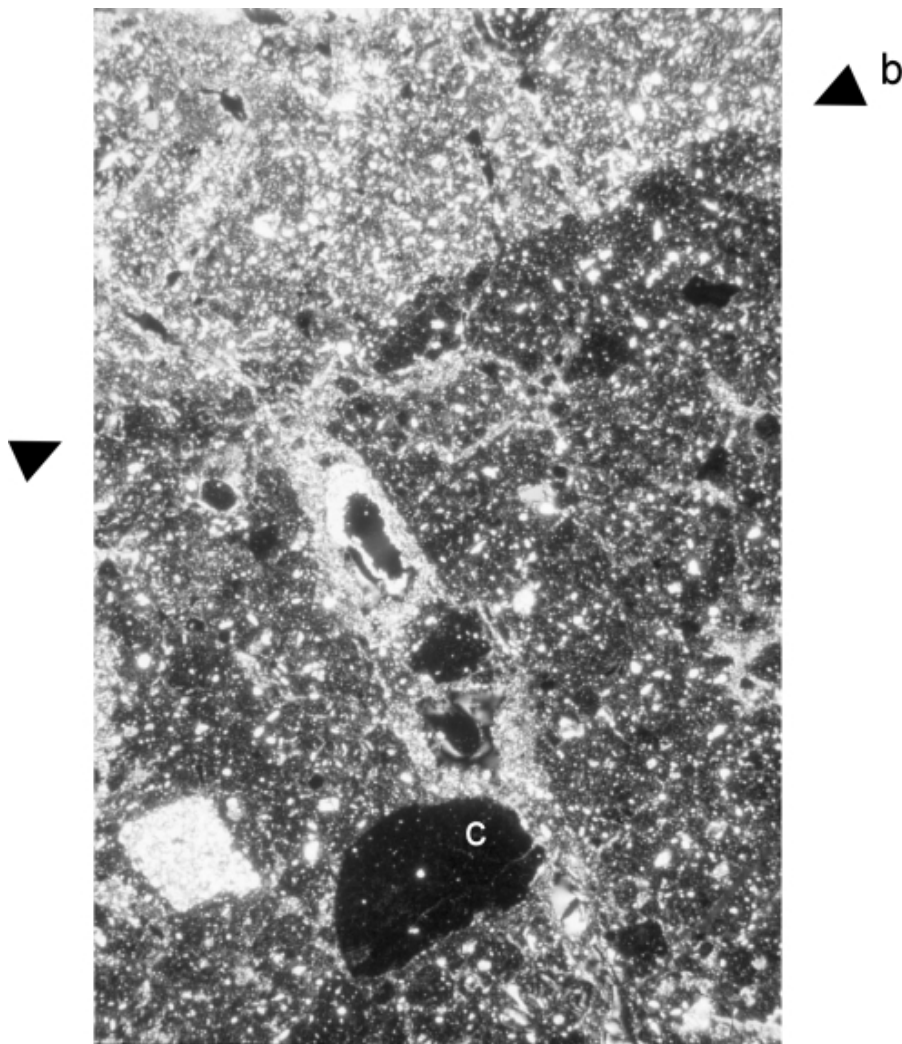


Figure 12. Photomicrograph showing the abrupt boundary (b) between layers 3 and 4. At the bottom, carnivore coprolite fragment (c) in the isotropic phosphatized matrix of layer 4. Thin section M1.6, XPL. Frame length is 2.9 mm.

The lower boundary of layer 2 is diffuse and characterized by a granular microstructure with greater porosity (15–20%) compared to the underlying strata. The silty clay aggregates are similar to those of layer 3, but much more fragmented. The minor components of layer 2 are the same as those observed in layers 3 and 4, except for the presence of a coprolite fragment that contains some phytoliths. This coprolite is from an omnivore or herbivore.

Post-Depositional Features

Two types of illuviation features occur in the pores: brownish yellow microlaminated argillans, and silty sand infillings composed of washed and well-sorted grains (quartz, micas, and calcite; Figure 15). The argillans, present only in layer 4 and the upper third of layer 3 (sample M1.3), formed before the silty sand infillings and seem to come from suspended clays in a temporary water table. The silty sand

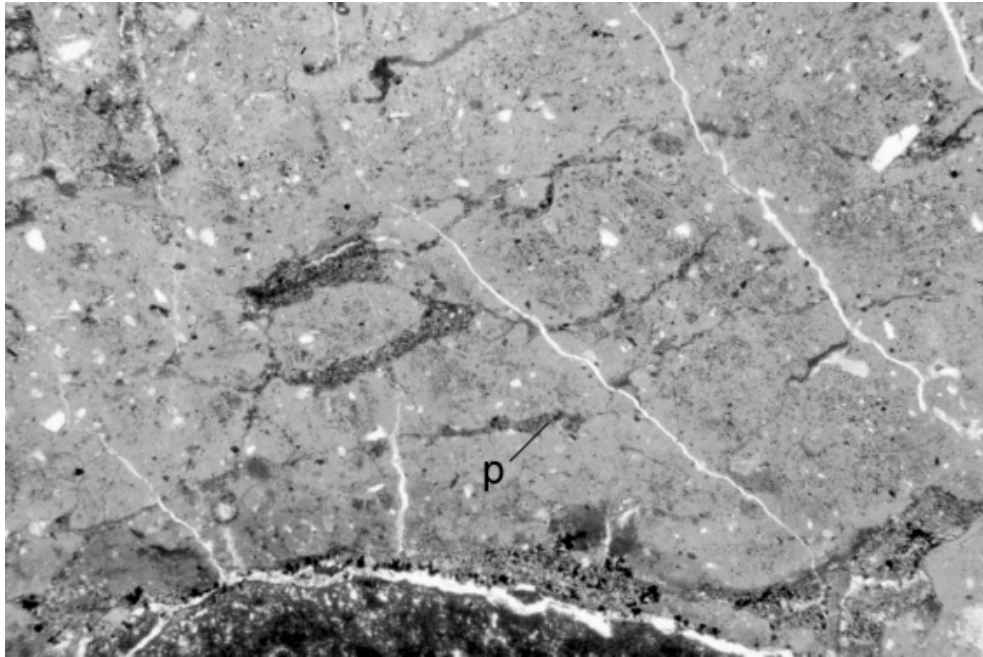


Figure 13. Photomicrograph showing subhorizontal platy structure (p) in layer 4 resulting from freeze-thaw processes. The space created by segregated ice was then filled with silty illuviation. Thin section M1.6, PPL. Frame length is 4.4 mm.

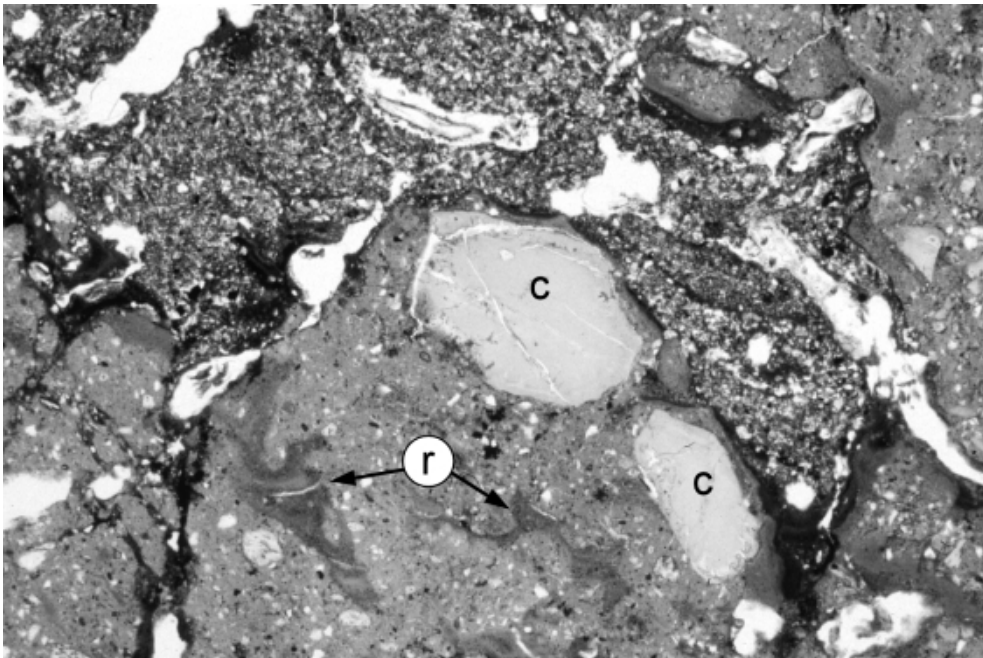


Figure 14. Photomicrograph of layer 3 showing the heterogeneous inner microstructure of the aggregates. Presence of reworked coatings (r) and two coprolite fragments of carnivore, probably lynx (c). Silty illuviation at the top. Thin section M1.6, PPL. Frame length is 4.4 mm.

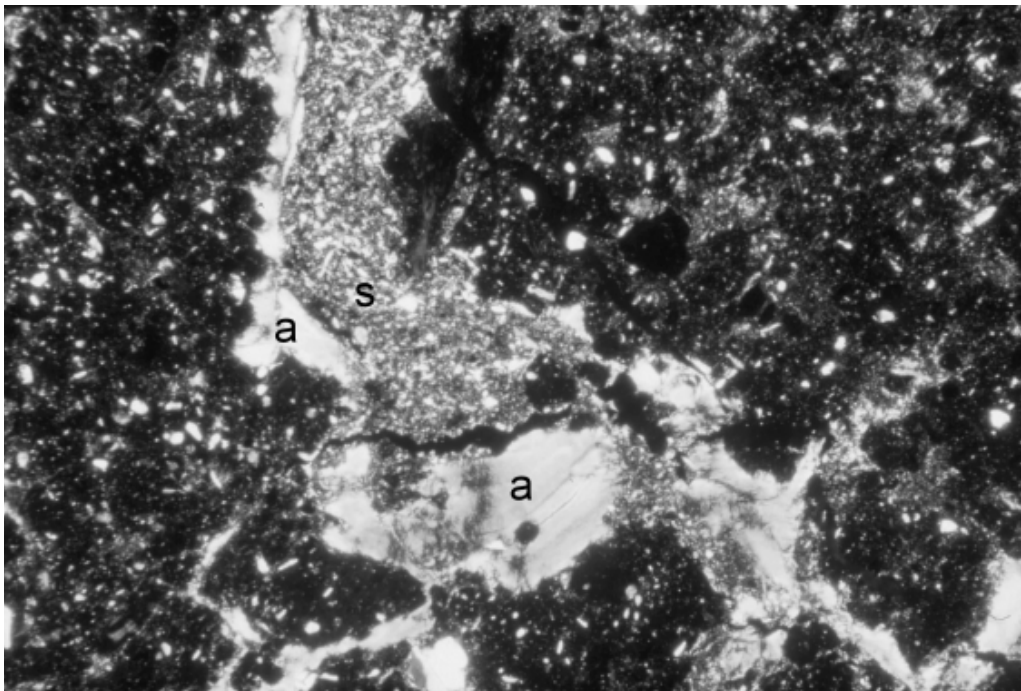


Figure 15. Photomicrograph showing microlaminated argillans (a) and washed, well-sorted silts (s) infilling a pore in layer 4. Thin section M1.6, XPL. Frame length is 2.2 mm.

infillings, present throughout the profile and especially in layer 2, probably developed by flushing that may have resulted from snow melt during the summer season.

DISCUSSION

The main goals of this study were to clarify the sedimentation dynamics of the rockshelter Sur-les-Creux, determine the composition of the fine sedimentary matrix, and explain the surprisingly round shapes of the gravels. Different conventional analytical methods, such as grain-size analysis and binocular study of bulk samples, were first applied and combined with micromorphology, which allowed identification of post-sedimentary processes and revealed an intense phosphatization of the sediment. Geochemistry and XRD analysis were then used to define the type and origin of the phosphates. The combination of these approaches has led to a general understanding of site formation processes and palaeoenvironmental conditions at Sur-les-Creux.

Deposition and Evolution of the Sediment

Most of the sediment in the Sur-les-Creux rockshelter comes from endokarstic sources. While the limestone of rockshelter is nondetrital, the fine fraction of the sediment contains many allochthonous silt grains, mainly quartz and micas. This fraction may be from loess deposits that were incorporated into the deposit's matrix through the karst network. Allochthonous, fine siliceous gravel also indicates such transport.

The calcareous gravels come either from deep karst or from the roof of the shelter. Gravels from deep karst are rounded, whereas fragments from the roof of the shelter are angular and of cryoclastic origin, representing the autochthonous fraction of the filling. The optical study of hand specimens revealed that no correlation exists between roundness and corrosion of the calcareous clasts. Chemical weathering related to pedogenesis is not sufficient to explain the rounding. Some angular fragments of cryoclastic origin are deeply corroded while other clasts, perfectly rounded by circulation in endokarstic channels, are hardly affected by dissolution.

The sediments of Sur-les-Creux accumulated in different phases that were relatively short compared to the hiatuses separating them. Layer 3, which also contains artifacts and bones, corresponds to a long period with a low sedimentation rate. The calcareous constituents evolved in the open-air and were strongly corroded. Based on this strong corrosion, we suggest that the sediments were affected by a humid and relatively temperate climate. During this period, the rockshelter was frequently occupied by cave bears (Schweizer, 2000). These bears, which disappeared from the Alps around 20,000 yr B.P., dug their lairs in the shelter, causing intense mixing of the sediments, as seen in the thin sections. From a micromorphological perspective, human occupation was only ephemeral. The rare artifacts found during excavation probably can be attributed to a late Mousterian occupation at the end of Middle Palaeolithic (Praz et al., 2000).

The palaeoclimatic, osteological, and archaeological evidence discussed above suggests that layer 3 formed during a long interstadial period that preceded the LGM, i.e., throughout the Middle Pleniglacial. Inputs from deep karst (layer 2) resumed later. Also recorded as a period when illuviation of silty sand occurred in pores, this rather humid phase may be related to the unplugging of the karst network at the end of the LGM or during the Late Glacial. In a final phase of rockshelter infilling, characterized by rather sporadic sedimentation (layer 1), only cryoclasts accumulated. This break up of the shelter's roof caused a retreat of the cliff, exposing the deposits to rainfall. Since the beginning of the Holocene, vegetation colonized its surface and pedological processes ensued.

Nature and Origin of Phosphates

The geochemical parameters within the rockshelter deposits reveal that the sedimentary substratum on which the rendzina developed was enriched in phosphates before pedogenesis began. Phosphatization thus took place well before pedogenesis. Furthermore, the high total phosphorus contents (nearly 50 mg/g at the bottom of the stratigraphic sequence) exclude an inheritance of phosphorus from the bedrock, which does not show any trace of this element.

The phosphates are essentially biogenic, and they are neomineralized within the sediment. The X-ray diffractometry points to a relatively well-crystallized phosphate of Ca F-apatite type. The detrital fraction is minor (maximum 10% of total phosphorus) and is related to bone and teeth fragments in the sediment; it is not

the product of allochthonous sources. In Sur-les-Creux, bone fragments do not show any traces of *in situ* alteration. Hence, they are not the source of the biogenic phosphate, which is contrary to the findings in the literature (Jenkins, 1992; Macphail and Goldberg, 1999).

Phosphorus originating from bird or bat guano can be rejected because of the nature of the cave. Although bats are common in central European karst systems (Abel and Kyrle, 1931), the depth of the Sur-les-Creux cave is not great enough to serve as a lair for them. This was confirmed by the osteological study, which identified no bones belonging to these species (Schweizer, 2000).

As suggested by the micromorphology, the intense phosphatization of the deposits at Sur-les-Creux implies addition of excrements and urine to the sediment. Coprolites of carnivores such as lynx, whose presence was deduced by archeozoological analysis, were identified in the rockshelter deposits, but in very low quantity. According to the osteological investigation, the cave bear is the major species present and seems to be responsible for most of the *in situ* phosphate. Unfortunately, not a single coprolite of these plantigrades could be identified under the microscope. However, this can be explained by taphonomical arguments. Cave bears were herbivorous, and produced coprolites poor in bio-minerals, which were therefore not likely to be preserved in the deposits (Rabeder et al., 2000). Also, modern brown bears (*Ursus arctos*) produce excrements that decompose very quickly, although their diet is more omnivorous than cave bears (B. Dahle, personal communication, 2002). This fact may explain the absence of *Ursus spelaeus* coprolites in caves of central and Western Europe (G. Rabeder and M. Pacher, personal communication, 2002). Another potential phosphate source to consider are carcasses of bears, since phosphate may represent as much as 2% of the living animal's weight (Schadler, 1931).

CONCLUSION

The results of our study suggest that the phosphates that have enriched the deposits of the Sur-les-Creux shelter have an essentially autochthonous origin related to colonization of the cave by bears. The seasonal but repeated presence of cave bear over a very long period explains the significant phosphate input, which comes mainly from excrements and urine, but probably also from carcass decomposition. Although less significant, lynx have also contributed to phosphatization of cave deposits through their coprogenic input.

From a methodological perspective, the conventional methods of micromorphology, sedimentology, and geochemistry provided both the basic and most significant results. Phosphorus sequential extraction, used to determine the type and origin of phosphates, also proved to be an effective method. However, it is important to note that only bulk sediment samples can be analyzed through this method. In future studies, we believe that chemical microanalysis (e.g., scanning electron microscopy, energy dispersive spectrometer, and mapping), coupled with micromorphology, has the potential to yield the best results.

We are grateful to Thierry Adatte and Federica Tamburini, who performed the XRD analyses, the phosphate speciation and the TOC dosage, and to André Strasser, who critically read a first version of the manuscript. We are also grateful to Thomas Beckmann, who made the thin sections, Beatrix Ritter for the grain-size analysis, and Xavier Pittet and Sandy Hämmerle, who helped with English translation. We gratefully acknowledge critical input from Paul Goldberg and Richard Macphail on various aspects of the study, and from Rolfe Mandel and Trina Arpin for editorial suggestions.

REFERENCES

- Abel, O., & Kyrle, G. (1931). Die Drachenhöhle bei Mixnitz. Wien: Österreichischen Staatsdruckereien.
- Adatte, T., Stinnesbeck, W., & Keller, G. (1996). Lithostratigraphic and mineralogic correlations of near K/T boundary clastic sediments in northeastern Mexico: Implication for origin and nature of deposition. In G. Ryder, D. Fastovsky, & S. Gartner (Eds.), *Special Paper 307* (pp. 211–226). Boulder, CO: Geological Society of America.
- Anderson, L.D., & Delaney, M.L. (2000). Sequential extraction and analysis of phosphorus in marine sediments: Streamlining of the SEDEX procedure. *Limnology, Oceanography*, 45, 509–515.
- Badoux, H., Chessex, R., Jeannet, A., Lugeon, M., & Rivier, F. (1960). Feuille 37: Monthey, Atlas géologique de la Suisse. Berne: Service Hydrologique et Géologique National.
- Bögli, A. (1980). Karst hydrology and physical speleology. Berlin: Springer-Verlag.
- Braillard, L. (2000). La dynamique de mise en place et l'évolution du remplissage de l'abri sous roche Sur-les-Creux à Tanay (Vouvry, VS). *Bulletin de la Murithienne*, 118, 41–58.
- Brochier, J.L., & Joos, M. (1982). Un élément important du cadre de vie des Néolithiques d'Auvernier Port: le lac. Approche sédimentologique. In A. Billamboz et al. (Eds.), *La station néolithique d'Auvernier-Port, cadre et évolution* (pp. 43–67), *Cahiers d'Archéologie Romande* 25. Lausanne: Bibliothèque Historique Vaudoise.
- Bullock, P., Federoff, N., Jongerius, A., Stoops, G., & Tursina, T. (1985). *Handbook for soil thin section description*. Wolverhampton: Waine Research Publishers.
- Campy, M. (1989). Etude sédimentologique du remplissage. In M. Campy, J. Chaline, & M. Vuillemeys, *La Baume de Gigny (Jura)*. Paris: Editions du CNRS.
- Courty, M.A., Goldberg, P., & Macphail, R. (1989). *Soils and micromorphology in archaeology*. Cambridge: Cambridge University Press.
- Deer, W.A., Howie, R.A., & Zussman, J. (1992). *An introduction to the rock-forming minerals* (2nd edition). London: Longman.
- Douglas, H.H. (1964). *Caves of Virginia*. Falls Church: Virginia Cave Survey.
- Dubois, A., & Stehlin, H.G. (1933). La Grotte de Cotencher, station moustérienne, *Mémoires de la Société Paléontologique Suisse* 52–53. Basel: Birkhäuser.
- Espitalié, J., Deroo, G., & Marquis, F. (1986). La pyrolyse Rock-Eval et ses applications. Partie 3. *Revue de l'Institut Français du Pétrole*, 41, 73–89.
- Giresse, P., & Van Vliet-Lanoë, B. (1986). Phosphatic mineralisation. In P. Callow & J. Cornford (Eds.), *La Cotte de St. Brelade 1961–1978* (p. 97). Norwich: Geo Books.
- Hadjouis, A. (1987). Granulométrie des fractions sableuses. In J.C. Miskovsky (Ed.), *Géologie de la Préhistoire* (pp. 413–426). Paris: Géopré.
- Hjulström, F. (1935). Studies on the morphological activities of rivers. *Bulletin of Geological Institution of Uppsala*, 25, 221–527.
- Jenkins, D.A. (1994). Interpretation of interglacial cave sediments from a hominid site in North Wales: translocation of Ca-Fe-phosphates. In A.J. Ringrose-Voase & G.S. Humphreys (Eds.), *Developments in Soil Science 22, Proceedings of the IX International Working Meeting on Soil Micromorphology*, Townsville, Australia, July 1992 (pp. 293–305). Amsterdam: Elsevier.
- Koby, F. (1938). Une nouvelle station préhistorique (paléolithique, néolithique, âge du bronze): Les cavernes de St. Brais (Jura bernois). *Verhandlungen Naturforschende Gesellschaft Basel*, 49, 138–196.

- Kübler, B. (1983). Dosage quantitatif des minéraux majeurs des roches sédimentaires par diffraction X. Cahiers de l'Institut de Géologie de Neuchâtel, Série AX , 1.1 and 1.2.
- Kübler, B. (1987). Cristallinité de l'illite, méthodes normalisées de préparations, méthodes normalisées de mesures. Cahiers de l'Institut de Géologie de Neuchâtel, Série ADX , 1.3.
- Kyrle, G. (1923). Grundriss der theoretische Speläologie. Speläologische Monographie. Wien: Österreichischen Staatsdruckereien.
- Lafargue, E., Espitalié, J., Marquis, F., & Pillot, D. (1996). Rocal-Eval 6, Applications in hydrocarbon exploration, production and soil contamination studies, Rock-Eval user manual. Rueil-Malmaison, France: Vinci Technologies.
- Lequatre, P. (1966). La grotte de Prélétang (commune de Presles, Isère). Le repaire d'ours des cavernes et son industrie moustérienne. Gallia Préhistoire, 9, 1–83.
- Macphail, R.I., & Goldberg, P. (1999). The soil micromorphological investigation of Westbury Cave. In P. Andrews, J. Cook, A. Carrant, & C. Stringer (Eds.), Westbury Cave—the Natural History Museum excavations 1976–1984 (pp. 59–86). Bristol: Western Academic and Specialist Press.
- Macphail, R.I., & Goldberg, P. (2000). Geoarchaeological investigation of sediments from Gorham's and Vanguard Caves, Gibraltar: microstratigraphical (Soil micromorphological and chemical) signatures. In C.B. Stringer, R.N.E. Barton, & J.C. Finlayson (Eds.), Neanderthals on the edge (pp. 184–200). Oxford: Oxbow Books.
- Perrenoud, C. (1993). Origine et mise en place des paragenèses phosphatées de remplissages karstiques. Etude micromorphologique des sédiments de la Caune de l'Arago et de la Baume Bonne. Unpublished doctoral dissertation, Musée National d'Histoire Naturelle, Institut de Paléontologie Humaine, Paris, France.
- Praz, J.C., Curdy, P., Leuzinger, U., Leuzinger-Piccand, C., & Schweizer, M. (2000). Paléolithique alpin à Tanay (commune de Vouvry, VS). Annuaire de la Société Suisse de Préhistoire et d'Archéologie, 83, 25–35.
- Rabeder, G., Nagel, D., & Pacher, M. (2000). Der Höhlenbär, Thorbecke Spezies 4. Stuttgart: Jan Thorbecke Verlag.
- Rivière, A. (1977). Méthodes granulométriques. Techniques et interprétations, Collection techniques et méthodes sédimentologiques. Paris: Masson.
- Ruttenberg, K.C. (1992). Development of a sequential extraction method for different forms of phosphorus in marine sediments. Limnology, Oceanography, 37, 1460–1482.
- Schadler, J. (1931). Die Ablagerungen. In O. Abel & G. Kyrle (Eds.), Die Drachenhöhle bei Mixnitz (pp. 169–223). Wien: Österreichischen Staatsdruckereien.
- Schmid, E. (1958). Höhlenforschung und Sedimentanalyse. Schriften des Institutes für Ur- und Frühgeschichte der Schweiz, 13. Basel: Verlag des Institute für Ur- und Frühgeschichte.
- Schmid, E. (1961). Neue Ausgrabungen im Wildkirchli (Ebenalp, Kt. Appenzell), 1958/59. Ur-Schweiz, 25, 4–11.
- Schweizer, M. (2000). Etude du matériel osseux de l'abri de "Sur-les-Creux." In J.C. Praz & et al., Paléolithique alpin à Tanay (commune de Vouvry, VS). Annuaire de la Société Suisse de Préhistoire et d'Archéologie, 83, 32–35.
- Tamburini, F. (2002). Phosphorus in marine sediments during the last 150'000 years, exploring relationships between continental weathering, productivity and climate. Unpublished doctoral dissertation, University of Neuchâtel, Neuchâtel, Switzerland.
- Trimmel, H. (1968). Höhlenkunde. Braunschweig: Vieweg.
- Van Vliet-Lanoë, B. (1986). Micromorphology. In P. Callow & J. Cornford (Eds.), La Cotte de St. Brelade 1961–1978 (pp. 91–96). Norwich: Geo Books.